AGU PUBLICATIONS

Geophysical Research Letters

RESEARCH LETTER

10.1002/2014GL061265

Key Points:

- The 2013 North Korean explosion has a nonisotropic radiation
- The radiation is inconsistent with the spherically symmetric source model
- The asymmetry of the source is caused by a surrounding prestressed rock

Supporting Information:

- Readme
- Figure S1a
- Figure S1b
- Figure S2a
- Figure S2b
- Figure S3
- Table S1
- Table S2

Correspondence to:
V. Vavryčuk,
vv@ig.cas.cz

Citation:
Vavryčuk, V., and S. G. Kim (2014), Nonisotropic radiation of the 2013 North Korean nuclear explosion, *Geophys. Res. Lett.*, *41*, doi:10.1002/2014GL061265.

Received 18 JUL 2014
Accepted 24 SEP 2014
Accepted article online 29 SEP 2014

Nonisotropic radiation of the 2013 North Korean nuclear explosion

Václav Vavryčuk[1] and So Gu Kim[2]

[1]Institute of Geophysics, Academy of Sciences, Prague, Czech Republic, [2]Korea Seismological Institute, Goyang, South Korea

Abstract On 12 February 2013, North Korea conducted an underground nuclear test in the northeastern mountainous part of the country. The explosion reached magnitude $m_b = 5.1$ being recorded at most of seismic stations around the world and becoming one of the best ever recorded nuclear explosions in history. Similarly, as other nuclear explosions buried in Nevada, Kazakhstan, or China, the 2013 North Korean explosion is characterized by a significant nonisotropic radiation. This radiation is manifested by distinct SH and Love waves in the wave field and is inconsistent with the model of a spherically symmetric source. We show that the Love waves are not generated by a tectonic earthquake triggered on a nearby fault structures but produced by asymmetry of the explosive source caused by presence of deviatoric stress in the surrounding rock. The retrieved moment tensor of the 2013 explosion is characterized by the isotropic component of $57 \pm 5\%$, the double-couple component of $17 \pm 9\%$, and the compensated linear vector dipole component of $24 \pm 7\%$. The *P*, *T*, and *N* axes of the moment tensor are consistent with the principal axes of the regional tectonic stress in the Korean Peninsula. A comparison of waveforms and particle motions of the 2013 explosion and the previous North Korean nuclear explosion buried in 2009 indicates that the 2013 explosion was slightly more nonisotropic.

1. Introduction

On 12 February 2013, North Korea conducted an underground nuclear test in the northeastern mountainous part of the country. The test site was located by U.S. Geological Survey at latitude 41.096°N and longitude 129.078°E close to the test sites of the 2006 and 2009 nuclear explosions. Its yield was estimated by the Defense Threat Reduction Agency (DTRA, http://www.rdss.info/) to be 8–13 kt and the magnitude was $m_b = 5.1$, the explosion being stronger than that in 2009 with m_b of 4.7 or in 2006 with m_b of 4.1.

The highest quality recordings of the 2013 explosion were provided by stations of the neighboring countries with epicentral distances less than 1200 km: stations of the New China Digital Seismic Network, Japanese National Research Institute for Earth Science and Disaster Prevention (NIED) Hi-Net and F-Net Seismograph Networks and South Korea National Seismic Network (KMA). In the high-frequency records, the *Pn* and *Pg* waves dominate, while the *Sn* and *Sg* waves are of significantly smaller amplitudes than for earthquakes. The *Pn* and *Pg* dominance was observed also for the previous North Korean nuclear explosions [*Pasyanos et al.*, 2012]. Both the *P* and *S* phases form complex wave groups typical for wavefields excited by shallow sources, being characterized by strong coda waves generated at structural heterogeneities near the Earth's surface.

The true initial *P* wave polarity is difficult to identify at many stations. The *P* or *Pn* waves (depending on the epicentral distance) begin with a low-frequency wave of positive polarity as expected for an explosive source (see Figure 1a). This initial phase is, however, often indistinct and hardly visible. In short-period records at regional distances or in records at teleseismic distances filtered usually to increase the signal-to-noise ratio, the positive low-frequency initial pulse is practically absent and can be overlooked (see Figure 1b, station BAR in the frequency band of 1.5–10 Hz).

The explosion also generated surface waves visible in low-frequency records (Figure 2). The surface waves consist of both Rayleigh and Love waves. The presence of Rayleigh waves is expected but the presence of Love waves is rather curious because theory does not allow excitation of Love waves by radially symmetric sources [*Massé*, 1981]. The amplitude of the Love waves is significant and even comparable to that of the Rayleigh waves at some stations as demonstrated also on particle motions plotted in the transverse (*T*)-radial (*R*) coordinate system (Figure 3). The excitation of the Love waves can be studied by measuring the ratio

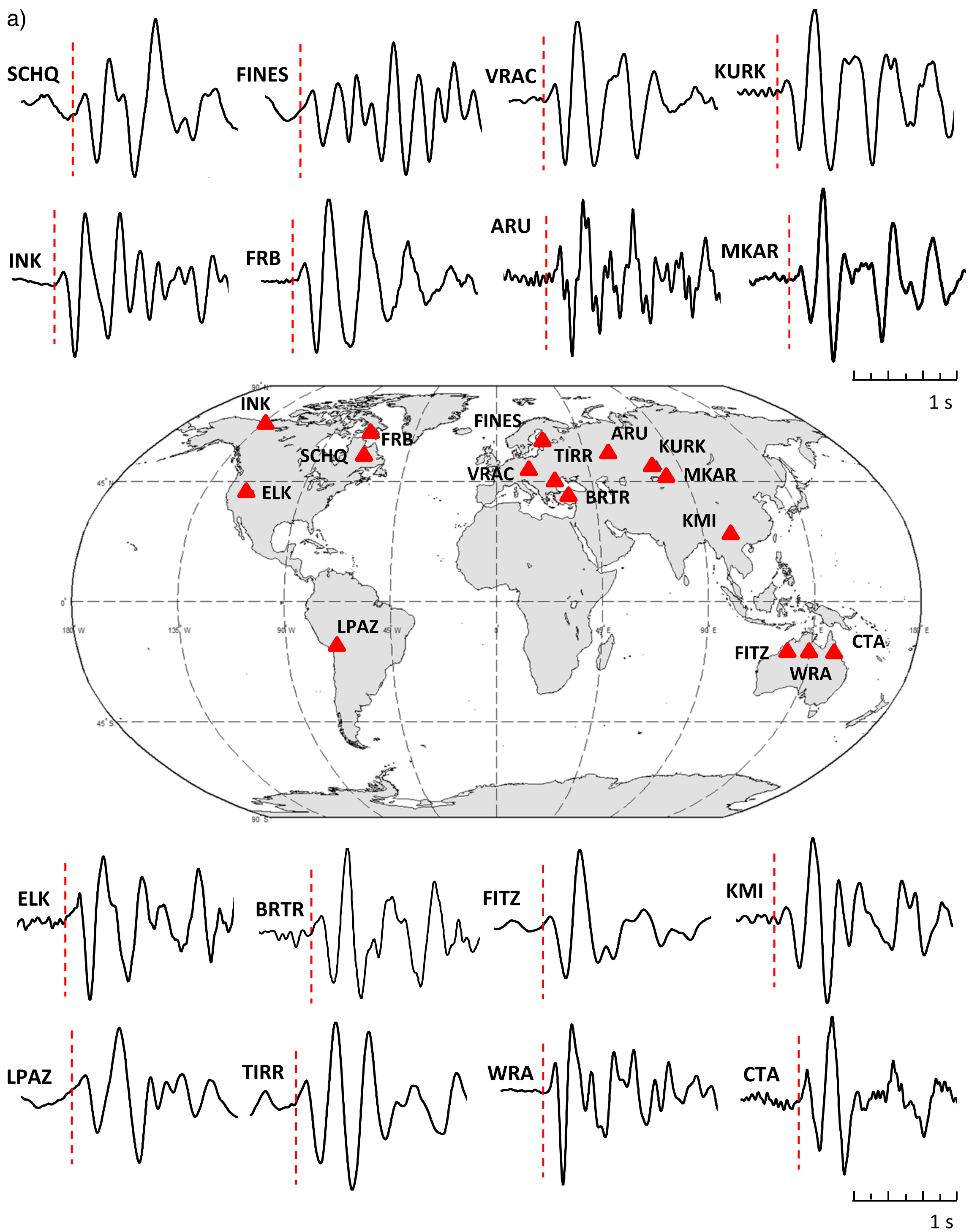

Figure 1. (a) Teleseismic *P* waveforms of the 2013 nuclear explosion recorded at selected stations around the world. The velocity records of the vertical component filtered by band-pass filter between 0.7 Hz and 5 Hz are displayed. The red dashed line marks the onset time. Notice a rather unclear and poorly visible positive initial motion at some stations. Time length of 6 s is displayed in seismograms. (b) (top) Map of the region and position of seismic stations at epicentral distances of less than 1500 km. (bottom) Vertical *P* velocity records at selected nearest stations displayed in two frequency bands: 0.5 Hz–10 Hz (first row) and 1.5 Hz–10 Hz (second row). The red dashed line marks the onset time. Notice the less visible positive first motion of the high-frequency signals (second row). Time length of 2 s is displayed in seismograms.

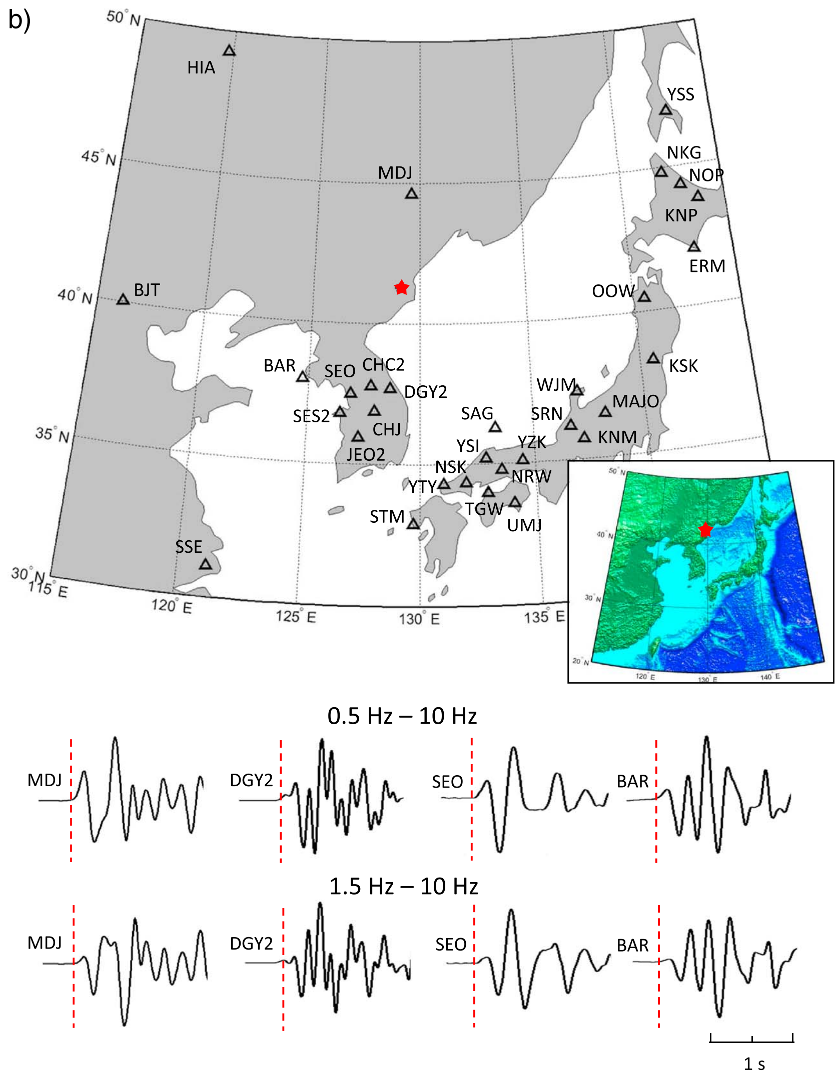

Figure 1. (continued)

of maximum amplitudes of the *T* and *R* components of surface waves at stations located in various azimuths to the explosion site. Analysis reveals that the *T*/*R* ratio is directionally dependent and forms a four-lobe pattern well known for radiation of the *S* or surface waves of tectonic earthquakes. This supports the evidence that the explosion is not symmetric and isotropic but must contain nonisotropic components.

2. Inversion for the Moment Tensor

The type of source and its focal mechanism can be determined from the moment tensor which describes equivalent body forces acting at a seismic source [*Aki and Richards*, 2002]. The moment tensor is usually decomposed into three components: the double-couple (DC), isotropic (ISO), and compensated linear vector dipole (CLVD) components. Shear faulting on a planar fault is represented by the DC component. A symmetric explosive source is described by the ISO component and tensile faulting, associated with opening or closing of a crack, is described by nonzero ISO and CLVD components [*Vavryčuk*, 2001, 2011]. More complicated sources can produce a moment tensor whose all three components, ISO, CLVD, and DC, are generally nonzero [*Julian et al.*, 1998].

The positive polarities of the initial *P* wave motion at stations around the world indicate that the isotropic part of the moment tensor is dominant. In order to determine the minor nonisotropic components, we have to invert for the full moment tensor. The complexity of high-frequency body waves at regional distances

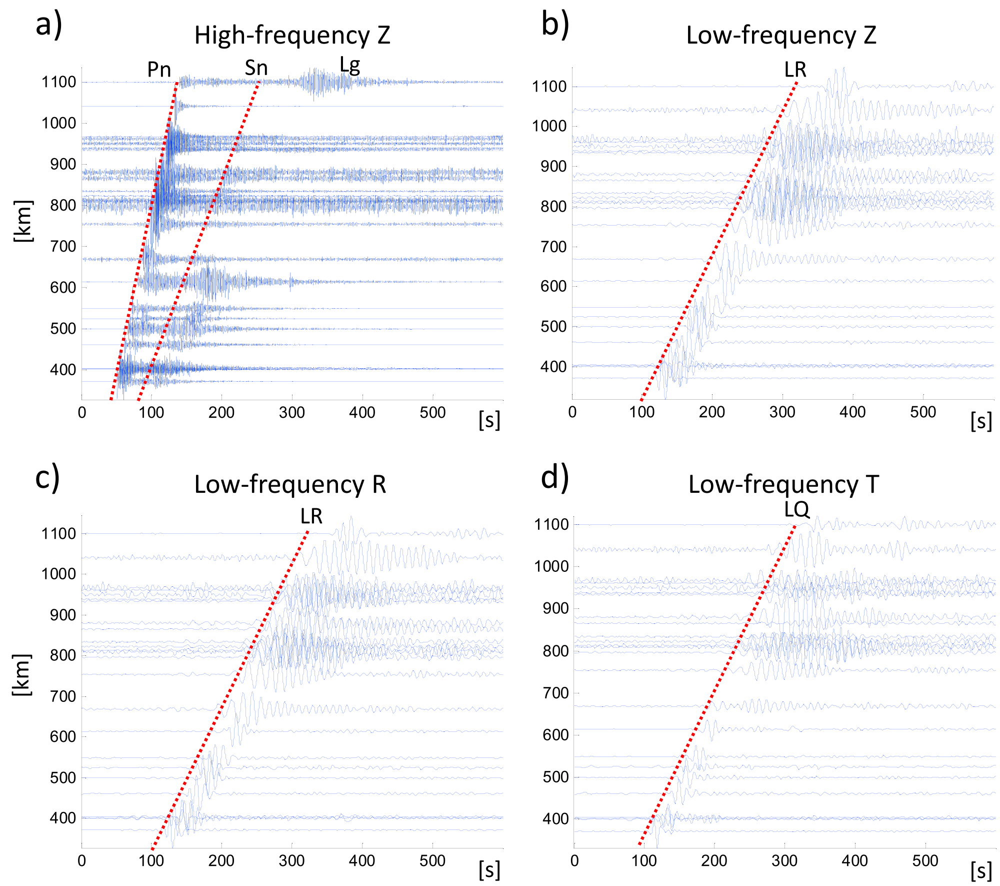

Figure 2. Velocity records at stations with an epicentral distance less than 1100 km. (a) High-frequency vertical records are displayed in the frequency band 0.7 Hz–5.0 Hz. (b) Low-frequency vertical, (c) radial, and (d) transverse records are displayed in the frequency band 0.04 Hz–0.10 Hz. Notice the significant amplitude of surface Love waves in the transverse component (Figure 2d) which is inconsistent with radiation of a radially symmetric source.

(hundreds to thousands of kilometers) and imperfect knowledge of the velocity model prevent using the body waves in the inversion. Instead, low-frequency surface waves can be exploited. When inverting waves in periods between 5 s to 100 s, it is sufficient to adopt a simple velocity model with several layers in the Earth's crust and upper mantle. In addition, rotating the records into the *R-T-Z* coordinate system, the inversion decouples into the inversion for the M11–M22 and M12 components of the moment tensor using Love waves and for the M11 + M22, M13, M23, and M33 components using Rayleigh waves [*Kanamori and Given*, 1981]. However, the individual components of the moment tensor are retrieved with different accuracy. In case of shallow sources, the highest accuracy is achieved for components M11, M22, and M12, while M13, M23, and M33 are, in general, not well resolved [*Kanamori and Given*, 1981; *Bukchin et al.*, 2010].

The moment tensor inversion was performed in two steps. First, the waveform inversion of surface waves was run using three-component records of 31 stations with epicentral distances of less than 1200 km (Figure 1b). The synthetic waveforms were calculated by the discrete wavenumber method [*Bouchon*, 1981]. Two velocity models were applied: a model with the continental crustal (see Table S1 in the supporting information) for the Chinese and Korean stations, published by *Kim and Kraeva* [1999], and a model with the oceanic crust (see Table S2) for the Japanese F-net stations. We inverted waves in frequency bands defined specifically for the individual stations. We tried to extend the frequency range of the inverted waves by incorporating high frequencies as much as possible in order to utilize more seismic information and stabilize the inversion. In this way, we succeeded in inverting the waveforms from the nearest stations distant less than 500 km in the frequency band 5 s–20 s, the more distant stations in the frequency bands 10 s–100 s or 20 s–100 s depending on the noise level in the records. A simple and robust time domain inversion was applied [*Sokos and Zahradník*,

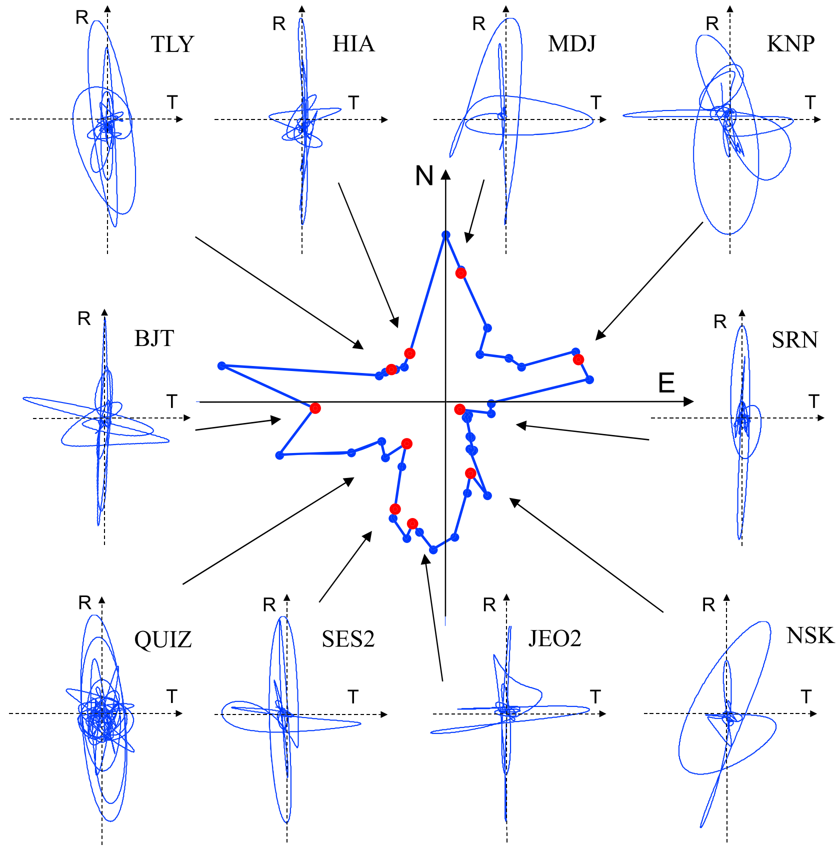

Figure 3. Directional variation of the ratio of maximum amplitudes of transverse (*T*) and radial (*R*) surface waves (blue dots) with examples of particle motions at selected stations (red dots). The velocity records were filtered in the frequency bands of 0.03 Hz–0.08 Hz (MDJ, SES2, and JEO2), 0.01 Hz–0.04 Hz (SRN, NSK, and NP), and 0.02 Hz–0.05 Hz (HIA, TLY, BJT, and QUIZ). The four-lobe pattern of the *T*/*R* ratio indicates the nonisotropic radiation of the explosion and its nonsymmetric character.

2008; *Vavryčuk and Kühn*, 2012]. The depth of the explosion was assumed to be alternatively 1 km and 2 km [*Gitterman et al.*, 2013]. In both cases, the fit of waveforms was high for optimum solutions with a variance reduction close to 0.7 (see Figures S1 and S2). The solutions yielded consistently a high positive isotropic component. The ISO percentages calculated according to the formulas of *Vavryčuk* [2001] were 55–60% and agreed with the observed positive *P* wave polarities. The DC percentage was about 20% for both explosions, but the CLVD percentage was more uncertain and displayed a high scatter (see Table 1).

In order to improve the accuracy of the CLVD component, we applied the second inversion step by fitting the *T*/*R* amplitude ratios of surface waves (i.e., the ratios of the Love/Rayleigh waves). The ratios were observed in an extended set of 43 stations with much better azimuthal coverage than the original set of stations (see Figures 3 and S3). The new set included 12 additional stations, which displayed either too complicated waveforms for fitting in the waveform inversion (epicentral distances between 1200 and 2500 km) or for which the amplification was not well known. Fitting the amplitude ratios is insensitive to errors in station

Table 1. Moment Tensor Solutions[a]

Method	M11	M22	M33	M12	M13	M23	ISO (%)	DC (%)	CLVD (%)	VR	RMS *ST*/*SR*
MTI (1 km depth)	4.66	6.53	5.42	−1.77	−1.26	−2.26	65.6	21.7	−12.6	0.67	0.56
MTI (2 km depth)	5.26	6.47	8.50	−1.36	0.17	−3.84	58.1	21.5	20.5	0.68	0.34
ST/*SR* inversion	5.38	5.79	9.93	−0.96	0.20	−4.01	56.6	16.6	23.9	0.68	0.20

[a]MTI – inversion of waveforms, *ST*/*SR* inversion – inversion of the *ST*/*SR* ratios, VR – variance reduction quantifying the fit between waveforms and synthetics, and RMS *ST*/*SR* – root-mean-square misfit of the *ST*/*SR* ratios. Components of the moment tensor are in $4*10^{15}$ Nm. The ISO, DC, and CLVD percentages are calculated according to formulas of *Vavryčuk* [2001].

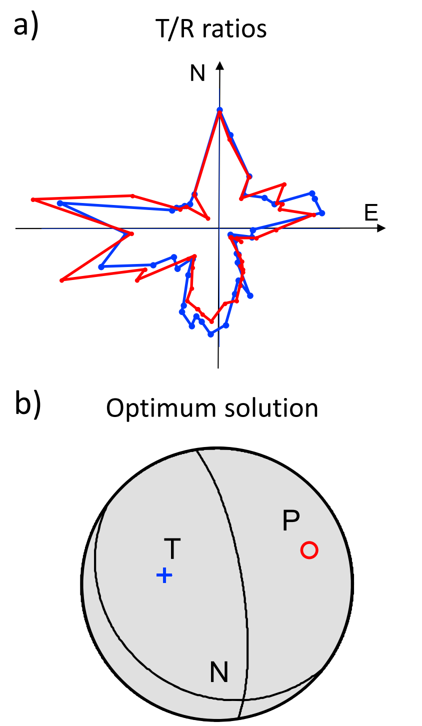

Figure 4. (a) Fit between the observed (blue) and synthetic (red) ratios of maximum amplitudes of the transverse (*T*) and radial (*R*) components of surface waves. (b) Final best fit solution found in the two-step moment tensor inversion. The solution is characterized by ISO = 57%, DC = 17%, and CLVD = 24%, see Table 1.

amplifications, and less sensitive to site effects, imperfect knowledge of the velocity model and of the depth of the explosion than the full waveform inversion. For these reasons, the amplitude ratios are often used, but mostly in the determination of focal mechanisms or moment tensors using body waves [*Snoke et al.*, 1984; *Jechumtálová and Šílený*, 2005]. The Love/Rayleigh wave ratios display similar advantages as the body wave ratios (e.g., *P*/*S* ratios), but their calculation is more laborious. Also, they are frequency and distance dependent and their interpretation is more involved.

The optimum solution was found by a grid search performed around the solutions found in the first inversion step. The retrieved solution is characterized by a positive isotropic component with ISO = 57 ± 5%. The *P* and *T* axes of the deviatoric moment tensors (Figure 4) are stable and the percentages of the DC and CLVD calculated using the formulas of *Vavryčuk* [2001] are 17 ± 9% and 24 ± 7%, respectively. The CLVD component is positive. The error bounds were calculated as standard deviations from 300 solutions with the RMS of the *ST*/*SR* ratios less or equal 0.25. The RMS value of the optimum solution was 0.20 (see Table 1).

3. Origin of the Nonisotropic Radiation

The observations of the Love waves generated by nuclear explosions point to their radially asymmetric nonisotropic radiation and have been reported by many authors, e.g., for the Nevada Test Site explosions [*Aki et al.*, 1969; *Toksöz et al.*, 1971; *Aki and Tsai*, 1972; *Wallace et al.*, 1983, 1985], for the explosions in Eastern Kazakhstan [*Helle and Rygg*, 1984], in China [*Zhang*, 1997], and also in North Korea [*Ford et al.*, 2009; *Murphy et al.*, 2013; *Barth*, 2014]. The excitation of Love waves (and *SH* waves) has been mostly attributed to tectonic stress release produced either by a triggered tectonic earthquake on a nearby fault [*Archambeau*, 1972] or by stress relaxation of the highly fractured zone immediately around the detonation point [*Archambeau*, 1972; *Harkrider*, 1977; *Minster and Suteau*, 1977]. However, the nonisotropic radiation of explosions can also have other origins [*Massé*, 1981]. A radially symmetric nonisotropic radiation (manifested by the presence of the vertically oriented CLVD) can be controlled by stress wave rebound, shock wave interaction with the free surface, and slap down of spalled near-surface layers [*Patton and Taylor*, 2011]. The radially asymmetric nonisotropic radiation (with the presence of the DC and CLVD of a general orientation) can partly be induced or affected by distinct Earth's topography close to the explosion site, tensile failure at depth [*Ford et al.*, 2009], effective or intrinsic seismic anisotropy in the focal zone [*Vavryčuk*, 2005], or by the nonspherical shape of the focal zone (e.g., expansion of an ellipsoidal instead of a spherical cavity) [see *Jin et al.*, 1997].

Although, nuclear explosions can occasionally trigger a tectonic earthquake [*Aki et al.*, 1969], this mechanism does not explain regular observations of nonisotropic radiation of nuclear explosions [*Massé*, 1981]. Interestingly, when we compare the waveforms of the 2009 and 2013 North Korean explosions, the idea of the nonisotropic radiation of the 2013 explosion caused by an induced tectonic earthquake can readily be excluded. The waveforms of both explosions are almost identical in all frequency bands except for the scale. The striking similarity of the waveforms of the 2013 and 2009 explosions (see Figure 5a) points to the same focus of both explosions and highlights some systematic and repetitive mechanism for generating the nonisotropic radiation. Apparently, it is quite unlikely that a tectonic earthquake could be induced in exactly the same manner (its magnitude, location, and origin time) for different explosions of a different yield.

Analyzing the remaining hypotheses, the interference of deviatoric tectonic stress in the rock with stress generated by the explosion seems to be the most likely origin of the nonisotropic radiation. The spherically symmetric dipole forces produced by the explosion and causing a sudden volume expansion interfere with the

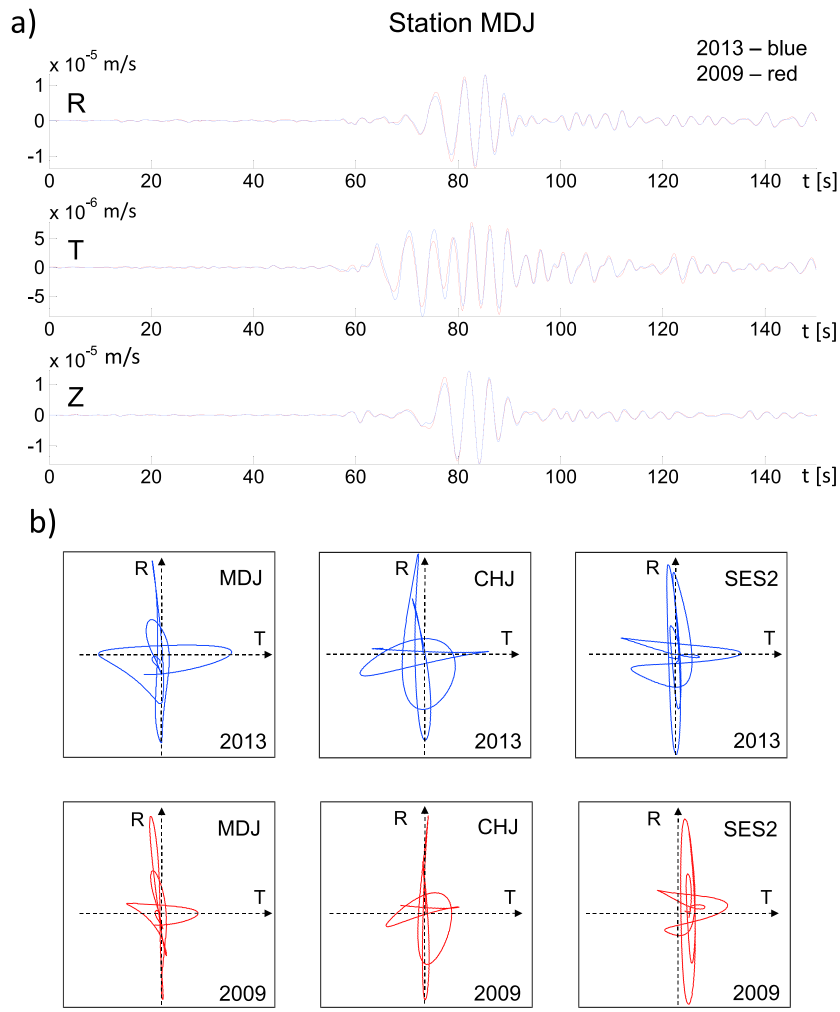

Figure 5. (a) Velocity records of the 2013 and 2009 explosions observed at station MDJ. The records were filtered in the frequency range of 0.02 Hz–0.25 Hz and rotated into the *R-T-Z* coordinate system. (b) *T-R* particle motions of surface waves of the 2013 and 2009 explosions at stations MDJ, CHJ, and SES2. The velocity records were filtered in the frequency range of 0.02 Hz–0.1 Hz. The *T*, *R*, and *Z* traces of the 2009 explosion in Figure 5a were multiplied by the scale factors: 2.56, 2.06, and 2.05, respectively.

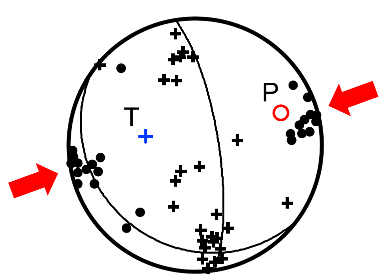

Figure 6. Comparison of the *P* (black dots) and *T* (black plus signs) axes of 27 earthquakes from the Korean Peninsula and its surrounding area with the optimum solution for the 2013 nuclear explosion. The red arrows show the maximum compression direction in the region. The *P* and *T* axes for the optimum solution of the explosion are marked by the red circle and blue cross, respectively. The 27 earthquakes from the period of 1936–2004 with $M \geq 4.0$ are taken from *Jin and Park* [2007].

deviatoric stress in the surrounding rock. The deviatoric stress in a compact rock can attain significant values ranging roughly from 20 to 40 MPa at depths between 1 and 2 km [*Brudy et al*., 1997]. Such stress conditions can remarkably distort the shape of the expanding cavity. The process is analogous to deforming a ball under a uniaxial pressure. Instead of a spherical shape of the cavity expected for an explosion buried in an unstressed medium, an ellipsoidal shape is more likely to be expected for an explosion buried in a prestressed medium. The major and minor axes of the ellipsoid will be along the minimum and maximum compression of tectonic stress, respectively. Consequently, the radiation of waves is no longer symmetric and the moment tensor is no longer isotropic. The three force couples describing the moment tensor will have no longer the same magnitude.

The idea of the stress-induced nonisotropic radiation of the explosion is supported by a comparison of the tectonic stress pattern in the Korean Peninsula and the retrieved moment tensor. Tectonic stress in the region was derived by *Jin and Park* [2007] from the GPS data and from fault plane solutions of prominent earthquakes with $M_w \geq 4.0$ in and around the Korean Peninsula from 1936 to 2004. The stress is rather uniform being characterized by the maximum compression in the ENE direction and the minimum compression in the NWN direction along a recent extension with back-arc basin formation in the East Sea/Sea of Japan [*Jin and Park*, 2007; *Barth and Wenzel*, 2010; *Murphy et al*., 2013]. A comparison of tectonic stress with the moment tensor of the 2013 explosion reveals that the direction of the maximum compression is consistent with the orientation of the *P* axis of the deviatoric part of the moment tensor (Figure 6). Moreover, the direction of the minimum compression is identical with the orientation of the *N* axis. The switch of the *T* and *N* axes of the deviatoric moment tensor can be produced by local stress conditions at the test site.

4. Discussion and Conclusions

The analysis of seismic records of 43 stations at regional distances proves that the 2013 explosion is nonisotropic. This is manifested by the presence of Love waves in the wavefield which display a typical four-lobe pattern known for tectonic earthquakes. The retrieved moment tensor is stable and rather insensitive to estimated depth of the explosion (in the depth range of 1–2 km). The ISO component prevails in the moment tensor attaining a value of 50–60%. The deviatoric component consists of the DC (10–25%) as well as the CLVD (15–30%). The *P*, *T*, and *N* axes are in directions similar to the principal directions of regional tectonic stress. This evidences that the nonisotropic radiation is related with tectonic stress in the surrounding rock rather than with shear faulting triggered along preexisting nearby fault structures. The deviatoric stress in the prestressed rock could attain values of 20 MPa or more. It caused probably an asymmetric shape of the cavity developed during the explosion and produced an asymmetric radiation of seismic waves.

The hypothesis of the stress-induced nonisotropic radiation predicts the generation of the Love waves also in the previous North Korean explosions. These explosions have been studied by *Ford et al*. [2009] and *Murphy et al*. [2013], who calculated their moment tensors and reported their nonisotropic radiation. The nonisotropic radiation of the 2009 and 2013 explosions was recently reported also by *Barth* [2014]. His moment tensors, however, suffer from poor accuracy. For the 2013 explosion, he obtained values: ISO = 32%, DC = 68%, and CLVD = 0% (calculated according to formulas of *Vavryčuk* [2001]) which predict negative *P* wave polarities for a large area on the focal sphere and thus contradict observations at stations at teleseismic distances (see Figure 1).

The comparison of waveforms and *T-R* particle motions of the 2009 and 2013 explosions in Figure 5 indicates that the focal mechanisms and moment tensors of the 2009 and 2013 explosions were very similar. We observe just minor differences in the *T-R* particle motions in Figure 5b pointing to systematically slightly lower amplitudes of the Love waves with respect to the Rayleigh waves in the 2009 explosion. This means that the 2013 explosion was slightly more nonisotropic than the 2009 explosion. This could have several origins. First, it could be caused by a different source extent of the 2009 and 2013 explosions. Assuming a similar depth of both explosions [*Gitterman et al*., 2013], the excitation of the Rayleigh waves of the 2013 explosion could have been more suppressed by nonlinear rheology of rocks near the Earth surface. Since the source size of the 2013 explosion was larger, this explosion could produce higher nonlinear deformations near the surface. These predominantly vertical deformations could absorb a significant part of elastic energy radiated in the Rayleigh waves. Second, if we assume that the 2009 and 2013 explosions were buried at different depths then the differences in the nonisotropic radiation could reflect different deviatoric stress at both foci. However, the striking similarity of waveforms of both explosions including high-frequency phases is rather against this assumption. And third, we should take into account that the 2013 explosion was buried in the rock massive partly damaged by the previous explosions. These explosions could form systems of cracks, predominantly tensile and oriented prevailingly along the maximum compression, which produced effective anisotropy in the focal zone. Subsequently, the 2013 explosion could form new crack systems but also reopen the existing preferentially oriented cracks. This could cause a more asymmetric source shape and a more nonisotropic radiation of the 2013 explosion notwithstanding the identical location to the 2009 explosion.

Acknowledgments
The data processed in this study have been provided by the South Korea National Seismic Network (KMA), the IRIS data center, the NIED F-net data center, and the DTRA Verification database. The data are available at these data centers upon request. We thank Douglas Dreger, Sean Ford, Raúl Madariaga, and one anonymous reviewer for their detailed and helpful reviews, Jan Švancara and Josef Havíř for help with acquiring the data from the USRK network, and Pavla Hrubcová for many inspiring discussions and for help with preparing the figures. This study was supported by the Grant Agency of the Czech Republic, project P210/12/1491.

Andrew Newman thanks Sean Ford and three anonymous reviewers for their assistance in evaluating this paper.

References

Aki, K., and P. G. Richards (2002), *Quantitative Seismology*, Univ. Science Books, Sausalito.

Aki, K., and Y. Tsai (1972), The mechanism of Love wave excitation by explosive sources, *J. Geophys. Res.*, *77*, 1452–1475, doi:10.1029/JB077i008p01452.

Aki, K., P. Reasenberg, T. DeFazio, and Y.-B. Tsai (1969), Near-field and far-field seismic evidences for triggering of an earthquake by the BENHAM explosion, *Bull. Seismol. Soc. Am.*, *59*, 2197–2207.

Archambeau, C. B. (1972), The theory of stress wave radiation from explosions in prestressed media, *Geophys. J.*, *29*, 329–366.

Barth, A. (2014), Significant release of shear energy of the North Korean nuclear test on February 12, 2013, *J. Seismol.*, *18*, 605–615.

Barth, A., and F. Wenzel (2010), New constraints on the intraplate stress field of the Amurian plate deduced from light earthquake focal mechanisms, *Tectonophysics*, *482*, 160–169.

Bouchon, M. (1981), A simple method to calculate Green's functions for elastic layered media, *Bull. Seismol. Soc. Am.*, *71*, 959–971.

Brudy, M., M. D. Zoback, K. Fuchs, F. Rummel, and J. Baumgärtner (1997), Estimation of the complete stress tensor to 8 km depth in the KTB scientific drill holes: Implications for crustal strength, *J. Geophys. Res.*, *102*, 18,453–18,475, doi:10.1029/96JB02942.

Bukchin, B., E. Clévédé, and A. Mostinskiy (2010), Uncertainty of moment tensor determination from surface wave analysis for shallow earthquakes, *J. Seismol.*, *14*, 601–614.

Ford, S. R., D. S. Dreger, and W. R. Walter (2009), Source analysis of the Memorial Day explosion, Kimchaek, North Korea, *Geophys. Res. Lett.*, *36*, L21304, doi:10.1029/2009GL040003.

Gitterman, Y., S. G. Kim, and R. Hofstetter (2013), Estimation source parameters of large-scale chemical explosions and recent underground nuclear tests, AGU Meeting, San Francisco, 9-13 December 2013.

Harkrider, D. G. (1977), Elastic relaxation coefficients for a spherical cavity m a prestressed medium of arbitrary orientation, *Geophys. J.*, *50*, 487–491.

Helle, H. B., and V. Rygg (1984), Determination of tectonic release from surface waves generated by nuclear explosions in eastern Kazakhstan, *Bull. Seismol. Soc. Am.*, *74*, 1883–1898.

Jechumtálová, Z., and J. Šílený (2005), Amplitude ratios for complete moment tensor retrieval, *Geophys. Res. Lett.*, *32*, L22303, doi:10.1029/2005GL023967.

Jin, P., G.-M. Xu, and W.-T. Lou (1997), Seismic moment tensor representations and radiation patterns in unbounded media with ellipsoidal cavities driven by low-frequency pressure, *Acta Seismol. Sinica*, *10*(5), 553–564.

Jin, S., and P. H. Park (2007), Tectonic activities and deformation in South Korea constrained by GPS observations, *Int. J. Geology*, *1*(2), 11–15.

Julian, B. R., A. D. Miller, and G. R. Foulger (1998), Non-double-couple earthquakes. 1: Theory, *Rev. Geophys.*, *36*, 525–549.

Kanamori, H., and J. W. Given (1981), Use of long-period surface waves for rapid determination of earthquake-source parameters, *Phys. Earth Planet. Inter.*, *27*, 8–31.

Kim, S. G., and N. Kraeva (1999), Source parameter determination of local earthquakes in Korea using moment tensor inversion of single station data, *Bull. Seismol. Soc. Am.*, *89*(4), 1077–1082.

Massé, R. P. (1981), Review of seismic source models for underground nuclear explosions, *Bull. Seismol. Soc. Am.*, *71*, 1249–1268.

Minster, J. B., and A. M. Suteau (1977), Far-field waveforms from an arbitrarily expanding, transparent spherical cavity in a prestressed medium, *Geophys. J.*, *50*, 215–233.

Murphy, J. R., J. L. Stevens, B. C. Kohl, and T. J. Bennett (2013), Advanced seismic analyses of the source characteristics of the 2006 and 2009 North Korean nuclear tests, *Bull. Seismol. Soc. Am.*, *103*(3), 1640–1661.

Pasyanos, M. E., W. R. Walter, and K. M. Mayeda (2012), Exploiting regional amplitude envelopes: A case study for earthquakes and explosions in the Korean Peninsula, *Bull. Seismol. Soc. Am.*, *102*(5), 1938–1948.

Patton, H. J., and S. R. Taylor (2011), The apparent explosion moment: Inferences of volumetric moment due to source medium damage by underground nuclear explosions, *J. Geophys. Res.*, *116*, B03310, doi:10.1029/2010JB007937.

Snoke, J. A., J. W. Munsay, A. G. Teague, and G. A. Bollinger (1984), A program for focal mechanism determination by combined use of polarity and SV-P amplitude ratio data, *Earthquake Notes*, *55*(3), 15.

Sokos, E., and J. Zahradník (2008), ISOLA—A Fortran code and Matlab GUI to perform multiple point source inversion of seismic data, *Comput. Geosci.*, *34*, 967–977.

Toksöz, M. N., K. C. Thomson, and T. J. Ahrens (1971), Generation of seismic waves in prestressed media, *Bull. Seismol. Soc. Am.*, *61*(6), 1589–1623.

Vavryčuk, V. (2001), Inversion for parameters of tensile earthquakes, *J. Geophys. Res.*, *106*(B8), 16,339–16,355, doi:10.1029/2001JB000372.

Vavryčuk, V. (2005), Focal mechanisms in anisotropic media, *Geophys. J. Int.*, *161*, 334–346.

Vavryčuk, V. (2011), Tensile earthquakes: Theory, modeling and inversion, *J. Geophys. Res.*, *116*(B12), B12320, doi:10.1029/2011JB008770.

Vavryčuk, V., and D. Kühn (2012), Moment tensor inversion of waveforms: A two-step time-frequency approach, *Geophys. J. Int.*, *190*, 1761–1776.

Wallace, T. C., D. V. Helmberger, and G. R. Engen (1983), Evidence of tectonic release from underground nuclear explosions in long-period *P* waves, *Bull. Seismol. Soc. Am.*, *73*(2), 593–613.

Wallace, T. C., D. V. Helmberger, and G. R. Engen (1985), Evidence of tectonic release from underground nuclear explosions in long-period *S* waves, *Bull. Seismol. Soc. Am.*, *75*(1), 157–174.

Zhang, J. (1997), Source characterization using simplified waveforms: Tests on earthquakes and nuclear explosions in Xinjiang, China, *Bull. Seismol. Soc. Am.*, *87*(4), 832–846.